physica status solidi

pss

www.pss-journals.com

reprint

WILEY-VCH

Phys. Status Solidi B **252,** No. 3, 538–544 (2015) / **DOI** 10.1002/pssb.201451259

physica status solidi b
www.pss-b.com
basic solid state physics

Testing conditions for reversibility of martensitic transformations with an isotropic potential for identical particles

M. F. Laguna*

Centro Atómico Bariloche and CONICET, 8400 Bariloche, Río Negro, Argentina

Received 27 May 2014, revised 8 September 2014, accepted 20 October 2014
Published online 14 November 2014

Keywords atomistic model, martensites, numerical simulations, phase transformations

* e-mail lagunaf@cab.cnea.gov.ar, Phone: ++54 2944 44 5100, int. 5345, Fax: ++54 2944 44 5299

A simple interparticle potential for a set of classical identical particles is used to model martensitic transformations in two dimensions. The influence of the symmetry of the phases involved in the transformation on the reversibility of such process is analyzed. Numerical simulations are used to confirm the theoretical suggestion that a necessary condition for reversibility is that transformations be group–subgroup.

1 Introduction Martensitic transformations (MT) are diffusionless shear transformations. These displacive first-order solid–solid transitions take place between a high-symmetry phase called austenite and a low symmetry (and usually also low temperature) one called martensite.

Such transformations have been found in many metals and alloys, but they are also present in some proteins and ceramic materials. From a theoretical point of view, the interest from this transformation comes from the fact that very elementary processes govern the main effects that these materials exhibit [1]. The MT is most commonly driven by mechanical deformation or by a change in temperature, and central to its phenomenology is the fact that, during the transformation, the atomic displacements are very small, typically lower than the interatomic distance. If the transformation is driven by temperature, different orientations of martensite are obtained from a single crystal austenite. They are called the *martensitic variants* and emerge from distortions of the austenite structure along different (but crystallographically equivalent) directions when the martensite is formed.

Some materials exhibiting MT posses the ability to recover their external shape upon thermal (or stress) cycling. In this case, the transformation is called "reversible," and paradigmatic systems presenting a reversible MT are the useful shape memory alloys [2]. Other materials, as steels, exhibit irreversible MT [3]. A question arises: what are the main factors determining this behavior?

One of the usual explanations for the irreversibility in some materials (iron based, among others) focuses in the change of volume that occurs during transformation, which causes stress and defects. However, there are some materials for which irreversibility is not associated to any change of volume [4].

An interesting suggestion is given in Ref. [5], where a mathematical theory is used to claim that a necessary condition for reversibility of an MT follows simply from symmetry relations between the parent and product phases: reversible martensites are such that both phases are related by a group–subgroup relation (because a unique parent lattice can be identified for every transformed product), whereas, irreversibility implies that such an identification is impossible or ambiguous.

These results suggest that both mechanisms, change of volume and symmetry, should contribute to the irreversibility of a martensitic transformation. Nevertheless, the complexity of real systems makes difficult to analyze both contributions separately. Moreover, realistic three-dimensional potentials display partial irreversibility in spite of group–subgroup relations between phases. This behavior can be attributed to topological defects, which appears when variants and twin structures grown in different directions. These kinds of potentials are closer to real systems, and also capture the complexity of the MT transitions in which several factors contribute. As will become clear below, the model used in this study (being 2D and exhibiting MT which

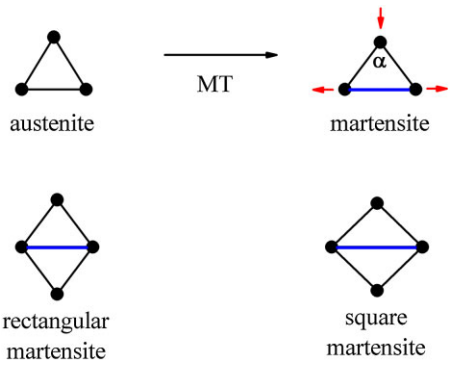

Figure 1 2D martensitic transformation described in this paper. Red arrows indicate the deformations applied at each segment, whereas, blue segment denotes the elongated side of the triangle. The three martensitic variants correspond to elongate one of the three sides of the triangle. The value of the angle α defines the geometry of the martensite: if $\alpha < \pi/2$ a rectangular martensite is obtained, whereas, $\alpha = \pi/2$ produces a square martensite.

almost no change of volume [6]) becomes an excellent candidate for studying the isolated effect of the symmetry in the reversibility of the transition.

The concept introduced by Bhattacharya and collaborators in Ref. [5] can be easily understood making use of a two-dimensional (2D) representation: the austenite phase is properly represented by a hexagonal (also called triangular) structure, and the martensitic variants can be associated with three equivalent deformations along the three sides of the triangle (see Fig. 1). When the angle α is less than $\pi/2$, the martensitic phase obtained has a rectangular (equivalent to the 3D rhombohedral) structure. The case $\alpha = \pi/2$ produces a square martensitic lattice. In the triangular–rectangular (T–R) MT, particle displacements are much lower than nearest neighbor distances. T–R MT is then reversible because each particle in the martensitic phase has a unique way to return to the parent triangular structure. On the contrary, the 2D triangular–square (T–S) MT is irreversible. In this case, particles in the square phase do not have a unique transformation path to go back to the austenite phase, because the displacements are such that particles in the martensitic phase are at the same distance of the two nearest places to move. When the transformation to the austenitic phase proceeds, they have two possibilities of forming the austenitic structure and hence they do not necessarily return to their initial positions.

The formal manner to express these ideas is the following: the rectangular lattice, belonging to the 2*mm* spatial plane group, is a subgroup of the 6*mm* symmetry group at which the hexagonal structure belongs. On the contrary, the symmetry group of the square martensite (plane group 4*mm*) is not a sub-group of the 6*mm* symmetry group of the hexagonal austenite [7]. This is enough to claim that this last transition is irreversible [5].

MT have been exhaustively explored, both experimentally and theoretically. Several mathematical models were constructed to study MT, most of them including different kind of particles interacting through complex potentials [8, 9]. However, such a complexity is not necessary to qualitatively describe an MT: a isotropic potential for identical particles can display multiple stable crystalline structures [10, 11] that can be in turn associated to the parent and product phases of the MT. Following this idea, we developed in a previous work a spherically symmetric two body classical potential by slightly modifying a 6–12 Lennard–Jones prototype [6]. Such a potential produces different crystalline configurations whose relative stability can change when some of the parameters of the model is varied. Such variation drives a martensitic transformation in the system, and several interesting effects associated to them can be analyzed [6, 12–14]. In Ref. [6] we showed that the T–R transformation displays the shape-memory effect, whereas, in the T–S transformation the shape-memory effect is absent.

Here, we use such simple model to analyze how the symmetry of the crystalline configurations connected by an MT affects the reversibility of such transition. We performed numerical simulations to verify if the T–R transformation is reversible and the T–S transformation is not. Our work shows that the suggestion of Ref. [5] about the irreversibility of group–nonsubgroup MT can be confirmed with a very simple model.

2 Model and numerical simulation details The interaction potential has a repulsive core at short distances and attractive tail at large distances. This potential is based in the standard Lennard–Jones (LJ) one, but some extra contributions are included in order to have ground state configurations other than the compact ones. In Ref. [6] we conducted a detailed description of the model. A potential that has the required properties is a sum of four terms, $V(r) = V_0 + V_1 + V_2 + V_3$, where the main contributions come from the first two terms.

The first one, $V_0 = A_0\,[1/r^{12} - 2/r^6 + 1]$, acts if $r < 1$ and is the repulsive part of a LJ potential. Its weight in the total potential is measured by the parameter A_0.

The quartic term $V_1 = [(r-1)^2(r+1-2c)^2/(c-1)^4] - 1$ contributes with the attractive part to the total potential and is different from zero if $r < r_c$.

The last two terms V_2 and V_3 were included to penalize the triangular lattice, and/or favoring the martensitic phase. The first one provides a small minimum of amplitude A_2 (centered at d_2), whereas the second one is a small maximum of amplitude A_3 centered at d_3:

$$V_2 = -A_2 \frac{(r - d_2 - s_2)^2 (r - d_2 + s_2)^2}{{s_2}^4}$$
$$(\text{acting if } d_2 - s_2 < r < d_2 + s_2),$$

$$V_3 = A_3 \frac{(r - d_3 - s_3)^2 (r - d_3 + s_3)^2}{{s_3}^4}$$
$$(\text{acting if } d_3 - s_3 < r < d_3 + s_3).$$

Then, $V(r)$ generates a family of isotropic potentials, each of one being fully determined by the set of parameters $P = \{A_0, A_2, A_3, c, d_2, s_2, d_3, s_3\}$. We have performed a search among several sets that, of course, do not exhaust all the possibilities, and we find the two set of parameters, which we consider adequate to describe T–R and T–S transitions. The set $P_1 = \{A_0, 0.003, 0.01, 1.722, 0.98, 0.04, 1.74, 0.2\}$ drives a T–R transition by changing the parameter A_0. We found a critical value $A_0^c = 0.067$, above which the minimum energy state corresponds to a triangular (T) structure of lattice parameter close to one. For $A_0 < A_0^c$, the minimum energy structure is a rectangular (R) lattice. Besides, the T–S transition is obtained from the set $P_2 = \{0.024, A_2, 0.01, 1.730, 0.98, 0.1, 1.74, 0.2\}$ with variable A_2. The transition value in this case is $A_2^c = 0.022$ (see details in Ref. [6]).

Since the triangular lattice is the high-symmetry (6*mm*) phase, the T structure is naturally identified with the austenite. Moreover, the R (2*mm*) and S (4*mm*) low-symmetry structures will be associated with the martensitic phases.

As we said, the martensitic variants in this model arise from deformations of the triangles forming the hexagonal parent phase. To determine whether some particle in the sample corresponds to austenite or martensite structures, the elongated side of each triangle is colored. Thus, triangular (not distorted) regions have no colored segments, whereas, each martensitic variant is identified by a different color. See an example in Fig. 2.

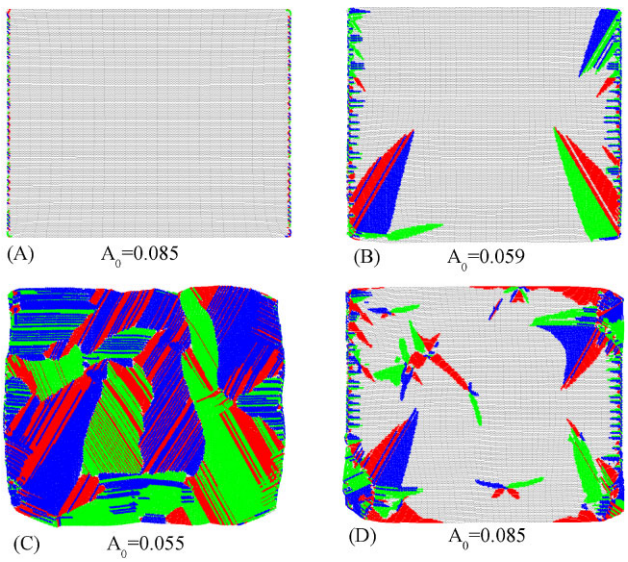

Figure 2 Snapshots of direct and reverse martensitic transformations. (A) Initial relaxed austenitic phase at $A_0 = 0.085$. Starting from this configuration, the value of A_0 is decreased at a constant rate $\Delta A_0 = 5 \times 10^{-9}$. (B) Beginning of the transformation at $A_0 = 0.059$. (C) Martensite obtained at $A_0 = 0.055$. From this structure, the reverse transformation is driven by applying an increase in A_0 at the same rate ΔA_0 as in the direct transformation. (D) Structure at $A_0 = 0.085$ in the process of retransformation.

Both, T–R and T–S transformations were numerically studied by solving the temporal dependence of the particle coordinates. We use the Verlet scheme and include a local friction term proportional to the velocities. Details of the implementation, which correspond to a zero temperature Langevin simulation, can be found in Ref. [6]. All the results showed in this work correspond to a system of $N = 40{,}000$ particles with open boundary conditions.

3 T–R reversible transition In a previous work, we showed that the T–R transition is reversible in a monocrystalline sample [6]. In the protocol used, the change of the parameter A_0, which drives the T–R transitions, was made in an abrupt manner because our goal was to determine the dependence of the typical grain size of the martensitic phase on the distance $A_0 - A_0^c$ from the value A_0^c at which austenite and martensite are in equilibrium. We found that deep quenches (i.e., higher values of $A_0 - A_0^c$) produce faster transformations and martensites with a much finer texture.

In this work, we are interested in understand how much the behavior previously observed is dominated by the way in which the parameter A_0 was changed. In order to study the transformation details, we repeated the transformation–retransformation process with a different protocol, in which a very slow change of A_0 is applied.

The initial condition consisted in a monocrystalline rectangular sample in a triangular structure. This configuration was allowed to relax through the dynamical algorithm at a value of A_0 for which austenite is stable. This relaxed configuration (shown in Fig. 2A) was the starting point from which the parameter A_0 was decreased at a constant rate. During the process, the evolution of the system was recorded as the T–R transformation proceeds. The first sign of the transformation is the nucleation of martensite variants at the edges of the sample. These nuclei grow, invading the interior of the sample, and it is also evident the existence of two variant wedge sectors, whose borders are the habit lines of the transformation (Fig. 2B). When the transformation is completed (Fig. 2C), the twinned martensite has practically disappeared. The number and size of the martensitic variants in the martensitic rectangular phase depends on the rate ΔA_0. This problem was addressed in our paper of Ref. [14] for the T–R transformation.

To model the retransformation to austenite, we reverse the previous conditions by slowly increasing A_0. In Fig. 2D a snapshot of the process can be observed, with several wedges and small regions of local deformation generated by interstitial particles. In some cases, these deformations remain in the system at higher values of A_0, even when the monocrystalline arrangement is recovered when A_0 reaches the region of stability of the austenite. This is the case of the austenite obtained at the rate $\Delta A_0 = 5 \times 10^{-9}$, which can be observed in Fig. 3A. Nevertheless, if the transformation is driven at a slower velocity, the final austenite does not display interstitial particles (see the austenite obtained for a rate $\Delta A_0 = 1 \times 10^{-9}$ in Fig. 3B). In any case, the configuration obtained after a complete transformation-

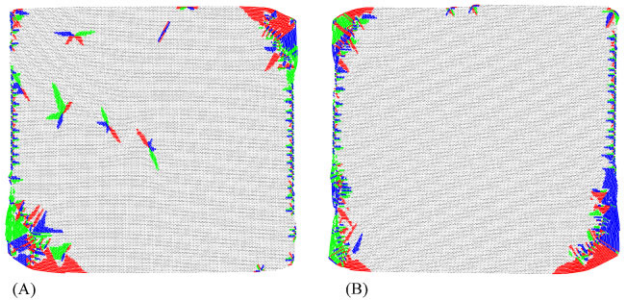

Figure 3 Final states obtained at two different rates. (A) $\Delta A_0 = 5 \times 10^{-9}$ and $A_0 = 0.137$. (B) $\Delta A_0 = 1 \times 10^{-9}$ and $A_0 = 0.121$. Note that, although interstitial particles are present in the first case, the austenite obtained is monocrystalline as the defects deform only locally the lattice.

retransformation cycle is composed by a single grain of monocrystalline austenite, presenting retained martensite at the borders of the sample.

A suitable manner to describe the behavior of the system during the transformation–retransformation process is by recording the temporal evolution of the fraction of particles in the martensitic phase, $\Phi_m = N_m/N$ (with N_m the number of particles belonging to one of the martensitic variants). In Fig. 4A, we show the evolution of Φ_m as a function of A_0 for the two rates previously described. The curves with open symbols correspond to the direct T–R transformations, whereas, full symbols indicate the reverse transformations, from the rectangular martensite to the triangular austenite. At the starting point ($A_0 = 0.085$) Φ_m is close to 0, indicating that almost all the system is in the austenitic phase, with the exception of a few particles located in the borders and corners of the sample. The value of Φ_m remains constant during the first steps of the process, consisting in the decrease of A_0 and a constant rate. When the parameter A_0 drops below its critical value, $A_0^c = 0.067$, the quick growth Φ_m indicate the beginning of the T–R transformation. For lower values of A_0, Φ_m reach the value one, indicating that the sample has transformed completely to martensite. The reverse transition starts from the martensitic phase obtained in the T–R transformation. The slow increase of A_0 gives rise to an abrupt decrease of Φ_m at a value $A_0 > A_0^c$. Note that, for the two cycles showed, Φ_m saturates at a value higher that one. This result is compatible with the retained martensites observed in Fig. 3A and B. The hysteretic behavior of this transformation was studied in Ref. [12].

To complete the description of the transition, we show in Fig. 4B the histograms of distances between particles for four configurations obtained during cycle of rate $\Delta A_0 = 5 \times 10^{-9}$. The histograms of panels (1)–(3), correspond to the snapshots of Fig. 2A, C and D, respectively. As expected, two characteristic distances are observed in the martensitic phase (see panel (2)), whereas, only one appears in the austenitic (triangular) phases. Note that at the point (4) the triangular structure was recovered in almost all the sample. As we increase A_0, the value of Φ_m continues to decrease slowly and the height of the triangular peak also grows with A_0 (not shown here).

The transformation–retransformation protocol was repeated for different values of the rate ΔA_0 and the same qualitative behavior was observed: (i) a polyvariant martensite is obtained at the end of the T–R transformation, whose structure depends on ΔA_0, and (ii) a monocrystalline austenite (with some elastic deformations and a few defects) is recovered at the end of the complete cycle.

These results confirm that the T–R martensitic transformation is reversible. As we first claim in Ref. [6], this behavior is a consequence of the way in which the T–R transformation proceeds: the particles displacements during the MT are much lower than the interparticle distance itself. Consequently, particles have a single way to coming back to the initial position. Moreover, the reversibility of the transition is the main cause of the shape memory effect in this simple model. This is one of the most striking effects observed in materials that suffer MT and, as was demonstrated in Ref. [6], an essential condition for this to happen is that the transformation be reversible.

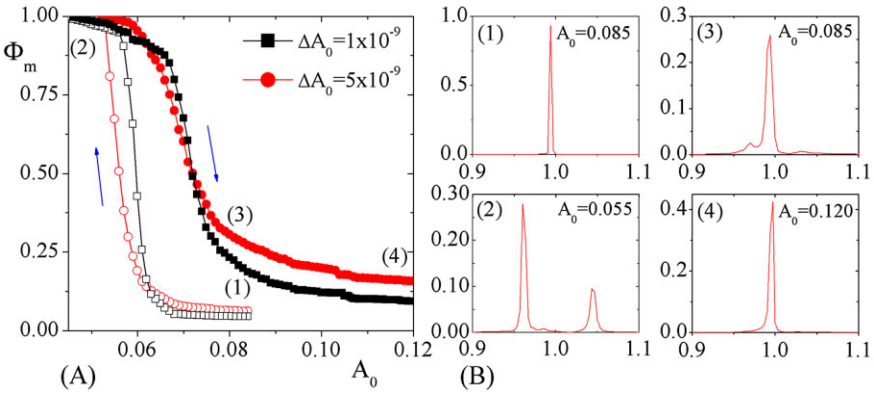

Figure 4 (A) Fraction of particles in martensitic phase as a function of A_0 for cycles at rates $\Delta A_0 = 1 \times 10^{-9}$ (in black) and $\Delta A_0 = 5 \times 10^{-9}$ (in red). Open symbols correspond to the T–R transformation, whereas full symbols indicate the reverse transformation. (B) Histograms of distances between particles for four points of the red cycle of panel (A).

4 T–S irreversible transition In the work, [6] we dedicated a few lines to the T–S transition. In that paper, we started with a value of the driving parameter for which the triangular phase is stable ($A_2 = 0.03$) and abruptly change A_2 to a value for which the square phase has lower energy. Using this protocol, the obtained martensitic state was a polycrystalline structure formed by grains of square phase in the three different orientations, related to the three possible deformations of the parent triangle. When the parameter A_2 was reversed to the initial value and letting the system evolve, a polycrystalline triangular structure was obtained, which retained some small grains of square phase.

Here, we explore in detail the T–S transition, implementing the protocol described in the previous section. In Figs. 5 and 6, we show the snapshots of two transformations at different rates, $\Delta A_2 = 1 \times 10^{-9}$ and 5×10^{-9}. In both figures, we note that the T–S transformation does not proceed as the T–R one: two variant wedge sectors (as the ones in Fig. 2B) are not observed here. Another clear difference is that the martensite obtained in the T–S transition is untwined. On the other hand, the final martensitic phase has a number of variants, which depends on the rate ΔA_2, as was also observed in the T–R transformation.

The reverse transition to the austenitic phase is triggered by an increase in A_2 at the same rates used in the T–R transformation. The final states obtained are shown in Fig. 7. Note that a polycrystalline austenite is obtained in both cases, as observed also in Ref. [6] for a different protocol.

The temporal evolution of the fraction of particles in the martensitic phase, Φ_m, is shown in Fig. 8A for the two rates ΔA_2 displayed previously. We analyzed the T–S forward and reverse transitions by observing this quantity in detail. Starting from a sample in the austenitic phase (for which $\Phi_m = 0$) we decrease the value of A_2 and observe that Φ_m have a quick growth at a value of A_2 lower than the critical one ($A_2^c = 0.022$), as expected from the hysteretic behavior that these systems display (see Ref. [12]). For lower values of A_2 the value of Φ_m saturates to a value close to one, indicating that the sample has transformed almost completely. The second part of the cycle starts from the martensitic square state obtained in the T–S transformation. The slow increase of A_2 gives rise to an abrupt decrease of Φ_m at a value $A_2 > A_2^c$. The hysteresis loops have comparable widths, indicating that the rates ΔA_2 used in the simulations are low enough to disregard non-equilibrium effects in the transformation process. We show in Fig. 8B the histograms of distances

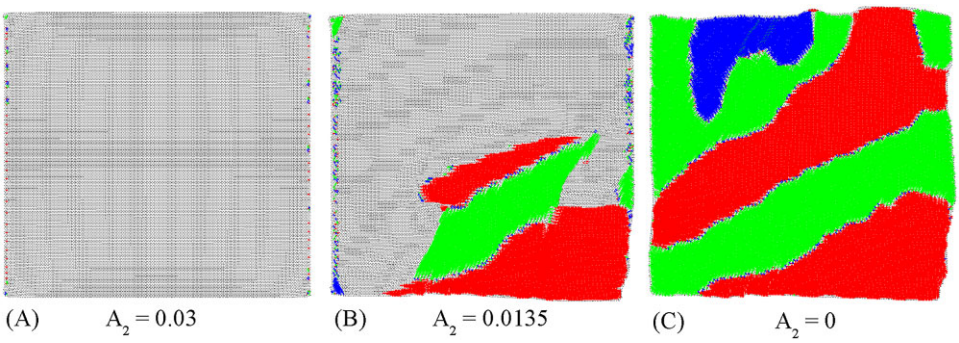

Figure 5 Snapshots of the T–S transition at a rate $\Delta A_2 = 1 \times 10^{-9}$. The value of A_2 is indicated in each panel. (A) Initial condition: triangular structure relaxed at $A_2 = 0.03$. (B) Beginning of the transition. (C) The final state is a square structure consisting of five grains of the three martensitic variants.

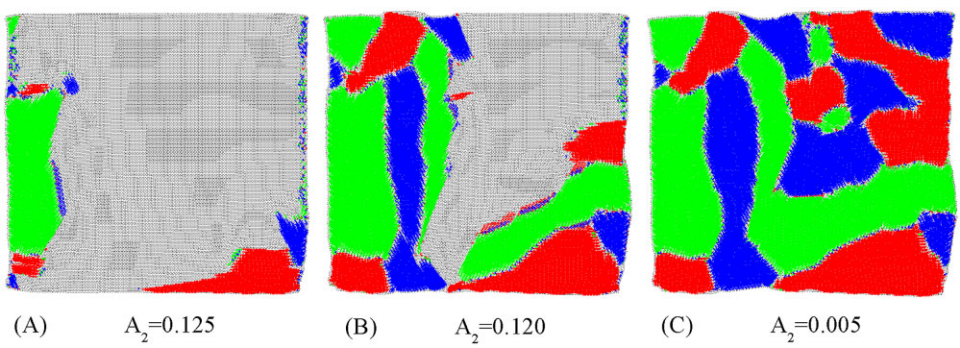

Figure 6 Snapshots of the T–S transition at a rate $\Delta A_2 = 5 \times 10^{-9}$. The value of A_2 is indicated in each panel. The initial condition is the same as Fig. 5A. (A) Beginning of the transition. (B) Growth of martensitic phase. (C) Final square structure consisting of sixteen grains of the three martensitic variants.

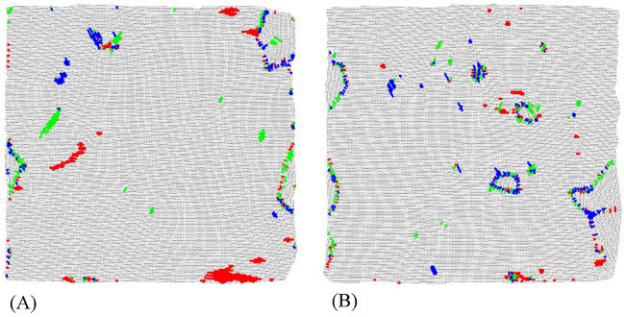

Figure 7 Snapshots of the final states of T–S transitions at two different rates. (A) $\Delta A_2 = 1 \times 10^{-9}$. (B) $\Delta A_2 = 5 \times 10^{-9}$. Note that in both cases austenitic grains of different orientation appear.

between particles for four configurations obtained during cycle of rate $\Delta A_2 = 5 \times 10^{-9}$. The histograms of panels (1) and (2) correspond to the first part of the cycle, and a clear T–S transition can be observed as A_2 decreases. As in the T–R transition, in the T–S one we observe two characteristic distances in panel (2), indicating the presence of a martensitic phase. Moreover, panels (3) and (4) correspond to the inverse transition. Note that at the point (3), for which $A_2 = 0.03$, the triangular structure was recovered and the triangular peak grows only slightly for higher values of A_2, as can be seen in panel (4). A further increase in A_2 does not change the situation observed in the panels (3) and (4).

In order to test the robustness of the results obtained for the T–S transition, we performed the transformation–retransformation protocol for different values of the rate ΔA_2 and obtained the same kind of results: (i) a sharp T–S transformation, at the end of which a polyvariant untwined martensite is obtained with a number of variants which depends on the rate ΔA_2; and (ii) a polycrystalline austenite when the reverse transition is completed.

In all the cases studied the final structure obtained after a complete cycle exhibit grains of triangular (austenitic) geometry of different orientation. The initial monocrystalline structure of Fig. 5A is always lost after the transformation–retransformation cycle, even when the distribution of distances clearly corresponds to a triangular phase. The polycrystalline structure obtained indicates that the T–S transformation is irreversible.

Moreover, and although it is beyond the purpose of this paper, numerical simulations were conducted of a square–triangular transition. The result is qualitatively the same as described in the triangular–square case: starting from an initial condition of square structure, and varying the parameter A_2 in order to bring the system to a region of parameters where the stable phase is the triangular one, the transformation occurs and the final structure is a polycrystalline phase with regions of different orientation, making the transition irreversible (not shown here).

5 Summary and conclusions Using an isotropic 2D potential devised for identical particles, the effect that the symmetry of the crystalline configurations connected by a martensitic transformation has on the reversibility of such transition was analyzed. Two sets of parameters were used, one producing a group–subgroup T–R transition and the other a group–nonsubgroup T–S transition. Both transformations have associated almost no change of volume [6] and this fact is one of the main strengths of the model, as it allows isolating the effect of the symmetry in determining the reversibility of the transition.

We performed numerical simulations using a protocol in which the parameters that drive the transformations are changed at a very slow and constant rate. We simulate the direct and reverse transition, performing cycles at different rates for the two transitions studied.

In the two cases, we analyzed the details of the process by observing snapshots of the particles during the process and the evolution of the fraction of particles in the martensitic phase. To check the structure of the configurations we construct histograms of the distances between particles in different stages of the transition.

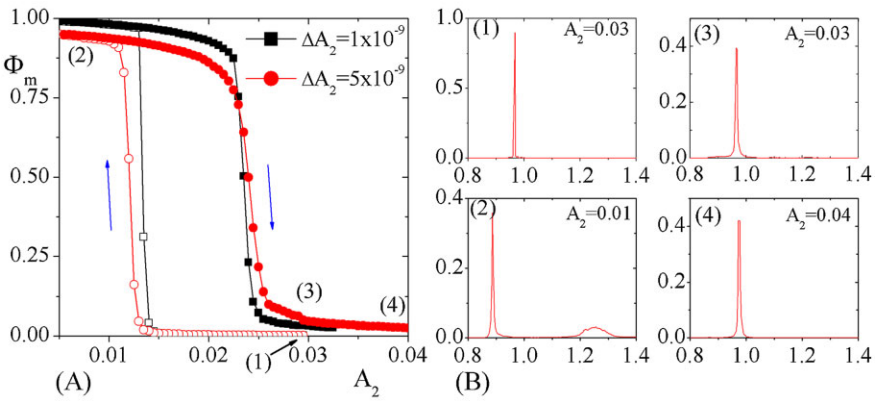

Figure 8 (A) Fraction of particles in martensitic phase as a function of A_2 for the rates of Figs. 5 and 6. Black square symbols correspond to $\Delta A_2 = 1 \times 10^{-9}$, whereas red circles indicate the cycle with $\Delta A_2 = 5 \times 10^{-9}$. Full symbols correspond to the forward T–S transformation, whereas open symbols indicate the reverse transformation. (B) Histograms of distances between particles for four points of the red cycle of panel (A).

For the group–subgroup T–R transition, a polyvariant martensite is formed at the end of the forward transformation, and a monocrystalline austenite with local elastic deformations appears at the end of the reverse transition. These results confirm the reversibility of this transition.

On the contrary, for the group–nonsubgroup T–S transition a polyvariant untwined martensite is obtained as a result of the direct transition, and a polycrystalline austenite after the reverse transition is ended. The lack of the initial monocrystalline austenite implies that this transition is irreversible.

The obtained results are in accordance with theoretical expectations [5] and demonstrate that elementary processes, which can be studied with very simple models, govern the main effects presented by materials exhibiting MT.

Acknowledgements M.F. Laguna acknowledges P. Arneodo Larochette, J. Andrade Gamboa and J.L. Pelegrina for the critical reading of the manuscript. This work was partially supported by the CONICET (PIP2011/0089) of Argentina.

References

[1] K. Bhattacharya, Microstructure of Martensite: Why it Forms and How It Gives Rise to the Shape-Memory Effect (Oxford University Press, Oxford, New York, 2003).
[2] K. Otsuka and C. M. Wayman, Shape Memory Materials (Cambridge University Press, Cambridge, 1998).
[3] G. B. Olson and W. Owen (eds.), Martensite (ASM International, Materials Park, OH, 1992).
[4] H. H. Lee, W.-Y. Jeong, and J. K. Kim, Macromolecules **35**, 785–794 (2002).
[5] K. Bhattacharya, S. Conti, G. Zanzotto, and J. Zimmer, Nature **428**, 55–59 (2004).
[6] M. F. Laguna and E. A. Jagla, J. Stat. Mech. **2009**, P09002 (2009).
[7] T. Hahn (ed.), International Tables for Crystallography, 2nd edition, Vol. A (IUCr, Kluwer Academic Publishers, Dordrecht, 1989), p. 780.
[8] J. Bhattacharya, A. Paul, S. Sengupta, and M. Rao, J. Phys.: Condens. Matter **20**, 365210 (2008).
[9] O. Kastner, Continuum Mech. Thermodyn. **15**, (5); 487–502 (2003).
[10] E. A. Jagla, Phys. Rev. E **58**, 1478 (1998).
[11] M. C. Rechtsman, F. H. Stillinger, and S. Torquato, Phys. Rev. Lett. **95**, 228301 (2005).
[12] M. F. Laguna and E. A. Jagla, in: ESOMAT 2009 – 8th European Symposium on Martensitic Transformations (EDP Sciences, 2009), doi: 10.1051/esomat/200902021
[13] M. F. Laguna and E. A. Jagla, Solid State Phenom. **172–174**, 73–78 (2011).
[14] M. F. Laguna, I. García Aguilar, P. Arneodo Larochette, and J. L. Pelegrina, Mater. Sci. Forum **738–739**, 137–142 (2013).

